INTERNATIONAL JOURNAL FOR NUMERICAL METHODS IN ENGINEERING, VOL. 37, 323–342 (1994)

DYNAMIC ANALYSIS OF STRUCTURES WITH UNILATERAL CONSTRAINTS: NUMERICAL INTEGRATION AND REDUCTION OF STRUCTURAL EQUATIONS

RIMANTAS BARAUSKAS

Department for Mechanics, Kaunas University of Technology, Topoliu 2-27, 3031 Kaunas, Lithuania

SUMMARY

Structural dynamic equations with unilateral constraints upon the displacements, velocities and accelerations are employed in order to represent vibrating elastic structures with normal, oblique impact and friction interaction points.

For obtaining a numerical integration scheme the Lagrange multipliers and a minimum work approach are employed at each time step. The algorithm is presented as an extension of the generalized Newmark scheme. It seems to retain the asymptotic features of the original one.

The reduction of the number of dynamic degrees of freedom of the unilaterally constrained structures is carried out by representing the equations of motion in modal co-ordinates of the unconstrained structure and truncating the dynamic contributions of higher modes.

The presented techniques have been verified by investigating free longitudinal vibroimpact motion laws of an elastic vibroconverter and free longitudinal and bending vibration of a vibroconverter interacting with a moving rigid body by oblique impact and friction forces.

1. INTRODUCTION

Impact contact behaviour arises in many machine parts, such as meshing gears, rolling bearings, clutches, etc. On the other hand, the operation of some mechanical systems is based upon the vibroimpact and sliding friction interaction of an elastic piezoelectric or magnetostrictive vibroconverter with an output link—the vibromotors and vibrodrives.[1]

Numerical integration of equations of motion implies that a structural behaviour is obtained by solving dynamic equilibrium equations at each time step. However, elastodynamic contact problems cannot be approached by requiring only a dynamic equilibrium of a unilaterally constrained structure at the post-impact time point. It is necessary to take into account finite velocity changes during the initial instant of a contact interaction of the points carrying finite masses. In References 2 and 3 the momentum conservation principle has been applied for each pair of contacting masses; however, the approach is valid for the lumped mass matrices rather than the consistent ones. Finite element meshes highly refined in the vicinity of a contact area have been employed in order to diminish amounts of mass taking part in a contact interaction directly.[4] Alternatively repulsive contact forces have been represented as non-linear functions of mutual penetration of contacting surfaces into each other by employing rheological models of a contact surface.[1,5,6]

0029–5981/94/020323–20$15.00

Received 10 January 1992
Revised 15 April 1993

The numerical integration algorithm based upon the combination of the Lagrange multipliers and a minimum work approach to satisfy the constraints upon displacements and velocities has been presented in References 7 and 8. It works with consistent as well as with lumped mass matrices, a local impact condition being prescribed in terms of a velocity restitution coefficient.

Great amounts of computer resource necessary in order to obtain a transient response can be reduced by employing efficient numerical schemes[9-11] or by reducing an effective number of the dynamic degrees of freedom (d.o.f.) of a model. It appears as natural to regard a constrained structure being presented in terms of dynamic substructures of the unconstrained one, as in Reference 12 for an elastoimpact problem. The substructure modal synthesis and modal truncation of substructures or of a whole structure retaining residual compliances can be employed in order to reduce an effective number of the dynamic d.o.f.[13-15] In References 7 and 8 such an approach has been extended to unilaterally constrained structures.

In this paper an efficient implicit numerical integration scheme for unilaterally constrained elastic structures has been obtained and presented as an extension of the generalized Newmark's scheme.[11] It seems to retain the main asymptotic features of the original scheme, though it has not been proved here but only illustrated by numerical examples. The dynamic reduction is carried out by representing the equations in modal co-ordinates of an unconstrained structure and truncating the dynamic contributions of higher modal components. As a result, a reduced dynamic equation of low dimension is obtained, the residual modal compliance being evaluated by a matrix manipulation before the numerical integration. In order to verify the validity of the approach, the results of free longitudinal impact vibrations of a beam vibroconverter obtained by integrating full and reduced dynamic equations are considered.

2. DIRECT INTEGRATION OF STRUCTURAL EQUATIONS WITH UNILATERAL CONSTRAINTS

Consider a small displacement dynamic contact problem presented as

$$[M]\{\ddot{U}\} + [C]\{\dot{U}\} + [K]\{U\} = \{R(t)\} \tag{1}$$

with constraints upon the displacements,

$$[P]\{U\} \leqslant \{d_0\} \tag{2}$$

where $[M]_{n\times n}$, $[C]_{n\times n}$ and $[K]_{n\times n}$ are the structural mass, damping and stiffness matrices, respectively, and $\{U\}_{n\times 1}, \{R\}_{n\times 1}$ are the vectors of nodal displacements and external forces. Constraint inequality (2) with the matrix $[P]_{p\times n}, p < n$, implies that the nodes of possible contact interaction are known in advance, where each jth row of the matrix $[P]$ contains the direction cosines of the unit vector normal to the contact surface in the vicinity of the jth pair of the contacting nodes and the elements of the vector $\{d_0\}$ represent the initial distances between the nodes.

2.1. *Applying Lagrange multipliers*

Let us start our consideration with a static problem obtained by omitting the time-dependent terms in (1) and by presenting it as a minimization problem:

$$\min(\tfrac{1}{2}\{U\}^{\mathrm{T}}[K]\{U\} - \{U\}^{\mathrm{T}}\{R\}) \quad \text{with constraint (2)} \tag{3}$$

By applying the Lagrange multiplier approach to problem (3), we obtain the equation system

$$\begin{aligned} [K]\{U\} + [P]^{\mathrm{T}}\{\lambda_0\} &= \{R\} \\ [P]\{U\} &= \{d_0\} \end{aligned} \tag{4}$$

where $\{\lambda_0\}$ is the Lagrange multiplier vector of dimension $p \times 1$. The solution of (4) reads as

$$\{\lambda_0\} = ([P][K]^{-1}[P]^{\mathrm{T}})^{-1}([P][K]^{-1}\{R\} - \{d_0\}) \tag{5}$$

$$\{U\} = [K]^{-1}\{R\} - [K]^{-1}[P]^{\mathrm{T}}([P][K]^{-1}[P]^{\mathrm{T}})^{-1}([P][K]^{-1}\{R\} - \{d_0\}) \tag{6}$$

The physical meaning of each component λ_{0j} of the vector $\{\lambda_0\}$ is the normal interaction force between the jth pair of the contacting nodes. Only non-negative values of λ_{0j} are considered by modifying the original ones as follows:

$$\lambda_{0j} = \begin{cases} \lambda_{0j} & \text{if } \lambda_{0j} \geqslant 0 \\ 0 & \text{if the reverse is true} \end{cases} \tag{7}$$

The zero values of λ_{oj} correspond to the inactive constraints. In order to find out exactly the set of active constraints, the components of the vector $\{\lambda_0\}$ are obtained iteratively. The physical meaning of the term $[P]^{\mathrm{T}}\{\lambda_0\}$ in (4) is the force, exhibited by a structure upon constraints.

In order to formulate properly the dynamic contact problem, it is not sufficient to add dynamic and damping terms to the first equation of system (4) only. In general, numerical integration of structural dynamics equations implies that the status of a structure at the next time-integration point is defined by the values of displacements, velocities, accelerations and, may be, higher time derivatives of displacements at the current time point, as well as, by an external force law. It follows that not only the displacements but also their time derivatives must match the contact interaction constraints. Therefore, the auxiliary constraints

$$[P]\{\overset{(k)}{U}\} = \{d_k\}, \quad k = 1, 2, \ldots, m \tag{8}$$

upon the velocities, accelerations, etc., are to be employed in the case when constraints (2) are active (i.e. when they are satisfied as an equality), where m is the order of a numerical integration scheme. Later it will be shown that specific values on the right-hand side vector $\{d_k\}$ are selected in order to represent various local impact conditions.

It follows from the latter consideration that the dynamic contact problem can be presented as

$$\begin{aligned} [M]\{\ddot{U}\} + [C]\{\dot{U}\} + [K]\{U\} + [P]^{\mathrm{T}}\{\lambda_0\} &= \{R\} \\ [P]\{U\} &\leqslant \{d_0\} \\ [P]\{\overset{(k)}{U}\} &= \{d_k\}, \quad k = 1, 2, \ldots, m \end{aligned} \tag{9}$$

We integrate (9) numerically. If at the time point $t + \Delta t$ some rows of the second matrix relation of (9) are satisfied as an equality, and corresponding rows of the third one are not satisfied for some values of k, the values of velocities, accelerations and higher time derivatives $\{\overset{(k)}{U}\}$ must be corrected.

Assume that velocities are corrected during the very short time interval Δt_s, in comparison with the integration step. The velocities at the start and end of this time interval are represented by $\{\dot{U}\}^-$ and $\{\dot{U}\} = \{\dot{U}\}^- + \Delta\{\dot{U}\}$. According to Carnot's theorem, the change of the kinetic energy of a structure by introducing a new constraint equals the kinetic energy of lost velocities

$\frac{1}{2}\Delta\{\dot{U}\}^{\mathrm{T}}[M]\Delta\{\dot{U}\}$. The loss of energy is caused by the work done by contact forces during the time interval Δt_s. The motion of the system corresponds to the minimum value of this work, or, what is the same, to the minimum change of the kinetic energy. At the end of the time interval $(t, t + \Delta t_s)$, the constraints upon velocities must be satisfied, i.e. it is necessary to solve the problem

$$\begin{aligned} &\min \tfrac{1}{2}\Delta\{\dot{U}\}^{\mathrm{T}}[M]\Delta\{\dot{U}\} \\ &\text{with the constraint } [P]\Delta\{\dot{U}\} = -[P]\{\dot{U}\}^{-} + \{d_1\} \end{aligned} \tag{10}$$

By applying the Lagrange multiplier approach to problem (10), we obtain the equation system

$$\begin{aligned} [M]\Delta\{\dot{U}\} + [P]^{\mathrm{T}}\{\lambda_1\} &= 0 \\ [P]\Delta\{\dot{U}\} &= -[P]\{\dot{U}\}^{-} + \{d_1\} \end{aligned} \tag{11}$$

the solution to which reads as

$$\{\lambda_1\} = ([P][M]^{-1}[P]^{\mathrm{T}})^{-1}([P]\{\dot{U}\}^{-} - \{d_1\}) \tag{12}$$

$$\Delta\{\dot{U}\} = -[M]^{-1}[P]^{\mathrm{T}}([P][M]^{-1}[P]^{\mathrm{T}})^{-1}([P]\{\dot{U}\}^{-} - \{d_1\}) \tag{13}$$

By differentiating with respect to time the first equation of (9) and writing the relations for accelerations similar to (10)–(13) for velocities, we obtain the Lagrange multipliers $\{\lambda_2\}$ and the acceleration corrections $\Delta\{\ddot{U}\}$ as

$$\{\lambda_2\} = ([P][M]^{-1}[P]^{\mathrm{T}})^{-1}([P]\{\ddot{U}\}^{-} - \{d_2\}) \tag{14}$$

$$\Delta\{\ddot{U}\} = -[M]^{-1}[P]^{\mathrm{T}}([P][M]^{-1}[P]^{\mathrm{T}})^{-1}([P]\{\ddot{U}\}^{-} - \{d_2\}) \tag{15}$$

Similarly, we obtain all $\{\lambda_k\}$ and $\Delta\{\overset{(k)}{U}\}$, $k = 3, \ldots, m$. Physically the Lagrange multipliers $\{\lambda_1\}, \{\lambda_2\}, \{\lambda_3\}, \ldots$ represent the normal impetus, normal forces, derivatives of normal forces, etc. They represent the action of constraints upon a structure during the time interval $(t, t + \Delta t_s)$.

It follows from relation (13) that the impetus of constraint forces in the global reference system during the time interval $(t, t + \Delta t_s)$ is obtained as

$$\{S_1\} = -[P]^{\mathrm{T}}\{S_{\mathrm{N}}\} = -[P]^{\mathrm{T}}([P][M]^{-1}[P]^{\mathrm{T}})^{-1}([P]\{\dot{U}\}^{-} - \{d_1\}) \tag{16}$$

The forces of constraints allowing the change in acceleration as (13) during the time interval $(t, t + \Delta t_s)$ are defined as

$$\{F_1\} = -[P]^{\mathrm{T}}\{F_{\mathrm{N}}\} = -[P]^{\mathrm{T}}([P][M]^{-1}[P]^{\mathrm{T}})^{-1}([P]\{\ddot{U}\}^{-} - \{d_2\}). \tag{17}$$

2.2. Numerical integration scheme

We obtain the relations for expressing the values of displacements and their derivatives at successive discrete time points on the basis of the mth order generalized Newmark's scheme[11] for obtaining the values $\{U\}_{t+\Delta t}, \{\dot{U}\}_{t+\Delta t}, \{\ddot{U}\}_{t+\Delta t}, \ldots, \{\overset{m}{U}\}_{t+\Delta t}$ at the time point $t + \Delta t$ employing the values $\{U\}_t, \{\dot{U}\}_t, \{\ddot{U}\}_t, \ldots, \{\overset{m}{U}\}_t$ at the time point t. By applying the Lagrange multipliers, the dynamic equilibrium equation of the generalized Newmark's scheme at the time point $t + \Delta t$ is presented as

$$\begin{aligned} [A](\{U\}_{t+\Delta t} - \{U\}_t) + [P]^{\mathrm{T}}\{\lambda_0\} &= [G] \\ [P]\{U\}_{t+\Delta t} &= \{d_0\} \end{aligned} \tag{18}$$

where $[A] = b_2^*[M] + b_1^*[C] + b_0^*[K]$ is the dynamic stiffness matrix, $\{G\} = \{R\}_{t+\Delta t} - ([M]\{q_2^*\} + [C]\{q_1^*\} + [K]\{q_0^*\})$ is the equivalent external force,

$$\{q_k\} = \sum_{j=k}^{m} \overset{j}{\{U\}}_t \frac{\Delta t^{j-k}}{(j-k)!}, \quad b_k = \beta_k \frac{\Delta t^{m-k}}{(m-k)!}; \quad \Delta\overset{k}{\{U\}} = \overset{k}{\{U\}}_{t+\Delta t} - \overset{k}{\{U\}}_t, \quad k = 0, 1, \ldots, m$$

$$b_k^* = b_k/b_s, \quad \{q\}_k^* = \{q\}_k - b_k^*\{q\}_s, \quad k = 1, 2, \ldots, m.$$

The values $\beta_0, \beta_1, \ldots, \beta_{m-1}$ are selected in order to submit the desired asymptotic features to the numerical scheme, and $\beta_m = 1$ is assumed. By solving (18) and correcting the velocities and higher time derivatives according to (12)–(15), the numerical integration relations are obtained as

$$[A]\Delta\{U\} = \{G\} - [P]^T\{\lambda_0\} \tag{19}$$

$$\{U\} = \{q\}_0^* + b_0^*\Delta\{U\} \tag{20}$$

$$\overset{(k)}{\{U\}}^- = \{q\}_k^* + b_k^*\Delta\{U\}, \quad \overset{(k)}{\{U\}} = \overset{(k)}{\{U\}}^- - [M]^{-1}[P]^T\{\lambda_k\}, \quad k = 1, 2, \ldots, m \tag{21}$$

where the Lagrange multiplier vectors are obtained from the relations

$$\{\lambda_0\} = ([P][A]^{-1}[P]^T)^{-1}([P][A]^{-1}\{G\} - \{d_0\}) \tag{22}$$

$$\{\lambda_k\} = ([P][M]^{-1}[P]^T)^{-1}([P]\overset{(k)}{\{U\}}^- - \{d_k\}), \quad k = 1, 2, \ldots, m \tag{23}$$

It is necessary to point out that the Lagrange multipliers $\{\lambda_0\}$ evaluate the average values of normal interaction forces during time-integration step, because their momentary values are infinite when finite mass points are interacting. The impetus of the normal interaction forces $\{S_N\}$ during the time-integration step Δt is approximately obtained as

$$\{S\}_N^{t+\Delta t} = \frac{\{F_N\}^t + \{\lambda_0\}^{t+\Delta t}}{2}\Delta t + \{\lambda_1\}^{t+\Delta t} \tag{24}$$

Normal forces $\{F_N\}$ ensuring the dynamic equilibrium at the time point $t + \Delta t$ are obtained as

$$\{F_N\}^{t+\Delta t} = \{\lambda_0\}^{t+\Delta t} + \{\lambda_2\}^{t+\Delta t} \tag{25}$$

The meaning of relations (15) and (16) is explained in Figure 1 where the increments of velocities, accelerations, etc., are assumed to occur during the time interval Δt_s significantly

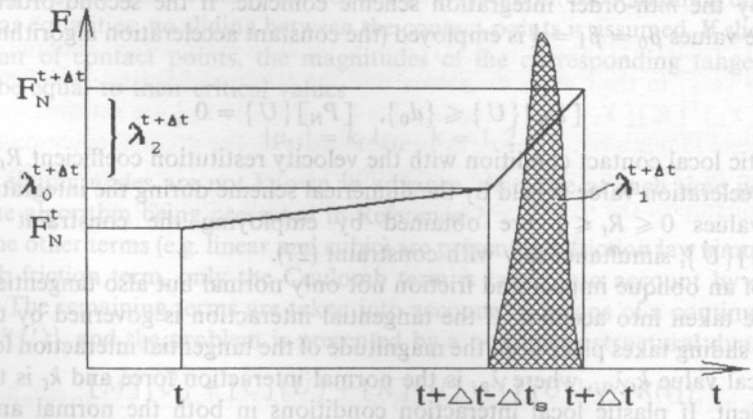

Figure 1. Interaction force and impetus time laws during the time integration step

shorter than the integration step. In general, if the number of constraints exceeds unity (i.e. the matrix $[P]$ contains more than one row), at each time point the active constraints must be determined iteratively using the following algorithm.

Algorithm

(1) At the current time step, obtain the values of the Lagrange multipliers $\{\lambda_k\}$, $k = 0, 1, \ldots, m$ by employing relations (22) and (23). Obtain the normal reaction impetus and forces $\{S_N\}$ and $\{F_N\}$ of the constraints by employing relations (24) and (25).
(2) Delete all the rows corresponding to the negative values of λ_{0j}, S_{Nj}, F_{Nj} from the constraint matrix $[P]$.
(3) If at the last execution of step 2, some rows have been deleted from the matrix $[P]$, go to step 1; else go to step 4.
(4) Obtain the values $\{\overset{(k)}{U}\}$, $k = 0, 1, \ldots m$, by employing numerical integration relations (19)–(21).
(5) Check if constraints (2) are satisfied, where the constraints deleted during the execution of step 2 also are to be taken into account. If all of them are satisfied by the vectors $\{U\}$ obtained during the execution of step 4, go to the next time-integration step; else include into the matrix $[P]$ all the rows corresponding to the unsatisfied constraints and go to step 1.

2.3. Application to structures with impact and friction interaction points

A general form of the normal impact local interaction condition is presented as

$$[P_N]\{U\} \leqslant \{d_0\}, \quad [P_N]\{\overset{(k)}{U}\} = \{d_k\}, \quad k = 1, 2, \ldots, m \tag{26}$$

where matrix $[P_N]$ contains the direction cosines of the unit vectors normal to the contact surfaces, vector $\{d_0\}$ represents the initial distances between interacting points, and vector $\{d_k\}$ is selected in order to represent properly the local impact condition. The values $\{d_k\} = 0$, $k = 1, 2, \ldots, m$ imply the plastic local impact, because the positions of the contact points in space as well as their velocities, accelerations and higher time derivatives of displacements taken into account by the mth-order integration scheme coincide. If the second-order Newmark's scheme with the values $\beta_0 = \beta_1 = \frac{1}{2}$ is employed (the constant acceleration algorithm, $m = 2$), the constraints

$$[P_N]\{U\} \leqslant \{d_0\}, \quad [P_N]\{\dot{U}\} = 0 \tag{27}$$

present an elastic local contact condition with the velocity restitution coefficient $R_f = 1$ because the constant acceleration value is held by the numerical scheme during the integration step. The intermediate values $0 \leqslant R_f \leqslant 1$ are obtained by employing the constraint $[P_N]\{\ddot{U}\} = -(1/\Delta t)R_f[P_N]\{\dot{U}\}_t$ simultaneously with constraint (27).

In the case of an oblique impact and friction not only normal but also tangential interaction forces are to be taken into account. If the tangential interaction is governed by the Coulomb friction law, no sliding takes place until the magnitude of the tangential interaction force does not exceed its critical value $k_f\lambda_{0j}$, where λ_{0j} is the normal interaction force and k_f is the Coulomb friction coefficient. If plastic local interaction conditions in both the normal and tangential directions are assumed and the second-order generalized Newmark's scheme is employed, the

constraints read as

$$[P_N]\{U\} \leqslant \{d_0\}, \quad [P_N]\{\dot{U}\} = 0, \quad [P_N]\{\ddot{U}\} = 0 \tag{28a}$$

$$[P_T]\{\dot{U}\} = 0, \quad [P_T]\{\ddot{U}\} = 0 \tag{28b}$$

where the matrix $[P_N]$ contains the direction cosines of the unit vectors tangential to the contact surfaces. In general, the matrix $[P_T]$ consists of two submatrices

$$[P_T] = \begin{bmatrix} P_{Tt} \\ P_{Tb} \end{bmatrix}$$

corresponding to two perpendicular directions on the contact surface, but here we restrict ourselves with two-dimensional problems by assuming $[P_{Tb}] = 0$.

By applying the Lagrange multiplier approach, the equations of motion of the structure with constraints (28) are presented as

$$[M]\{\ddot{U}\} + [C]\{\dot{U}\} + [K]\{U\} + [P_N]^T\{\lambda_0\} = \{R(t)\}$$
$$[P_N]\{U\} \leqslant \{d_0\} \tag{29}$$

$$[M]\Delta\overset{(k)}{\{\dot{U}\}} + [P_N]^T\{\lambda_k\} + [P_T]^T\{\mu_k\} = 0$$

$$[P_N]\Delta\overset{(k)}{\{U\}} = -[P_N]\Delta\overset{(k)}{\{U\}}^- \tag{30}$$

$$[P_T]\Delta\overset{(k)}{\{U\}} = -[P_T]\Delta\overset{(k)}{\{U\}}^-, \quad k = 1, 2$$

The physical meanings of the Lagrange multipliers in (29) and (30) are as follows: $\{\lambda_0\}$ are the normal forces, ensuring the coincidence of the contact points at the time point $t + \Delta t$, $\{\lambda_2\}$ the normal forces ensuring the corrections of acceleration values, $\{\lambda_1\}$ the impetus of normal forces, ensuring the corrections of velocity values, $\{\mu_2\}$ the tangential forces ensuring the corrections of acceleration values and $\{\mu_1\}$ the impetus of tangential forces, ensuring the corrections of velocity values.

At the current time-integration point, only the normal constraints corresponding to the positive values of the Lagrange multipliers $\{\lambda_0\}$ are taken into account in (29) by deleting the remaining ones from the consideration. Simultaneously, from (30) we delete the tangential constraints corresponding to the normal constraints deleted from (29). If all the remaining constraints in (30) are satisfied as equalities, no sliding between the contact points is assumed. If sliding takes place in the jth pair of contact points, the magnitudes of the corresponding tangential forces are assumed to be equal to their critical values

$$|\mu_{kj}| = k_f \lambda_{kj}, \quad k = 1, 2. \tag{31}$$

As a rule, sliding nodes are not known in advance, therefore at each time point iteration is necessary, the algorithm being presented in Reference 7.

When some other terms (e.g. linear and cubic) are present in a friction law simultaneously with the Coulomb friction term, only the Coulomb term is taken into account by employing constraints (28). The remaining terms are taken into account by means of a continuous function of velocities $\{V(\dot{U})\}$, and the problem is presented by a non-linear structural dynamic equation

$$[M]\{\ddot{U}\} + [C]\{\dot{U}\} + [K]\{U\} = \{V(\dot{U})\} + \{R(t)\} \tag{32}$$

with constraints (28).

3. DYNAMIC REDUCTION OF STRUCTURAL EQUATIONS WITH UNILATERAL CONSTRAINTS

For transient non-linear structural analysis it is desirable to deal with the models of possibly small dimension that enable one to obtain reliable results within reasonable computational costs. As a rule, the number of finite elements cannot be reduced because it is necessary to represent the local contact deformation properly. Here we present a unified approach to the reduction of the dynamic d.o.f. both of the linear and unilaterally constrained structures based upon the dynamic contribution truncation of higher modes of an unconstrained structure.

3.1. Linear structural equations

Consider structural equation of motion (1) with the proportional damping, i.e. $[C] = \alpha[M] + \beta[K]$. By solving the eigenproblem

$$([K] - \omega^2[M])\{U\} = 0 \tag{33}$$

we obtain eigenfrequencies ω_i, $i = 1, 2, \ldots, n$ and the matrix of eigenvectors $[Y] = [y_1, y_2, \ldots, y_n]$. The transfer to modal co-ordinates is carried out by means of the substitution

$$\{U\} = [Y]\{Z\} \tag{34}$$

where $\{Z\}$ is the modal displacement vector of a structure.

We split the vector of squares of eigenfrequencies into two subvectors

$$\begin{Bmatrix} \{\omega_1^2\} \\ \{\omega_2^2\} \end{Bmatrix}$$

and the matrix of eigenvectors into two submatrices $[Y] = [Y_1, Y_2]$. By truncating the dynamic and dissipative contributions of the modes corresponding to $\{\omega_2\}$, $[Y_2]$, equation (1) in modal co-ordinates is obtained as

$$\begin{aligned} [I]\{\ddot{Z}_1\} + [\mathrm{diag}(\mu_1)]\{\dot{Z}_1\} + [\mathrm{diag}(\omega_1^2)]\{Z_1\} &= [\Delta_1]^{\mathrm{T}}\{R\} \\ [\mathrm{diag}(\omega_2^2)]\{Z_2\} &= [\Delta_2]^{\mathrm{T}}\{R\} \end{aligned} \tag{35}$$

where $[\mathrm{diag}(\mu_1)]$, $[\mathrm{diag}(\omega_1^2)]$ and $[\mathrm{diag}(\omega_2^2)]$ denote the diagonal matrices containing the vectors $\{\mu_1\}$, $\{\omega_1^2\}$ and $\{\omega_2^2\}$ in their main diagonals, and the relations $[\mathrm{diag}(\mu_1)] = [Y_1]^{\mathrm{T}}[C][Y_1]$ $[\mathrm{diag}(\omega_1^2)] = [Y_1]^{\mathrm{T}}[K][Y_1]$ and $[\mathrm{diag}(\omega_2^2)] = [Y_2]^{\mathrm{T}}[K][Y_2]$ are satisfied.

Equation system (35) is a reduced one in comparison with the original equation (1). From the second equation of (35), the quasi-static correction $\{\tilde{U}\} = [Y_2]\{Z_2\}$ caused by the retained structural compliance of the dynamically truncated modes is obtained as

$$\{\tilde{U}\} = [S_k]\{R(t)\} \tag{36}$$

where

$$[S_k] = [Y_2][\mathrm{diag}(1/\omega_2^2)][Y_2]^{\mathrm{T}} = [K]^{-1} - [Y_1][\mathrm{diag}(1/\omega_1^2)[Y_1]^{\mathrm{T}} \tag{37}$$

If the stiffness matrix is singular, the approach proposed in Reference 15 can be applied in order to express $[S_k]$ without obtaining higher structural modes.

3.2. Structural equations with unilateral constraints

Consider structural dynamic equation (1) with unilateral constraints (2). By using the Lagrange multipliers, and by truncating the dynamic and dissipative contributions of the higher modes of the unconstrained structure we obtain

$$\begin{aligned}
[I]\{\ddot{Z}_1\} + [\mathrm{diag}(\mu_1)]\{\dot{Z}_1\} + [\mathrm{diag}(\omega_1^2)]\{Z_1\} &= [Y_1]^{\mathrm{T}}(\{R\} - [P]^{\mathrm{T}}\{\lambda\}) \\
[\mathrm{diag}(\omega_2^2)]\{Z_2\} &= [Y_2]^{\mathrm{T}}(\{R\} - [P]^{\mathrm{T}}\{\lambda\}) \qquad (38) \\
[P][Y_1]\{Z_1\} + [P][Y_2]\{Z_2\} &= \{d_0\}
\end{aligned}$$

Physically, the Lagrange multipliers $\{\lambda\}$ represent the normal interaction forces produced by constraints upon a structure. They are obtained as

$$\{\lambda(Z_1)\} = ([P][S_k][P]^{\mathrm{T}})^{-1}([P][Y_1]\{Z_1\} + [P][S_k]\{R\} - \{d_0\}) \qquad (39)$$

Only non-negative values of $\{\lambda\}$ are allowed; therefore, they are to be modified by means of the relation (7). By substituting (39) into the first equation of (38), we obtain the reduced dynamic equation

$$\begin{aligned}
[I]\{\ddot{Z}_1\} + [\mathrm{diag}(\mu_1)]\{\dot{Z}_1\} + ([\mathrm{diag}(\omega_1^2)] + [Y_1]^{\mathrm{T}}[\bar{P}]^{\mathrm{T}}[A]^{-1}[\bar{P}][Y_1])\{Z_1\} \\
= [Y_1]^{\mathrm{T}}([I] - [\bar{P}]^{\mathrm{T}}[A]^{-1}[\bar{P}][S_k])\{R(t)\} \qquad (40)
\end{aligned}$$

where $[A] = [\bar{P}][S_k][\bar{P}]^{\mathrm{T}}$ and $[\bar{P}]$ denotes the matrix $[P]$, from which the rows corresponding to zero values of λ_i are deleted, i.e. only the constraints active at the time point t are represented by the matrix $[\bar{P}]$. The reduced equation (40) contains the term

$$-[Y_1]^{\mathrm{T}}[\bar{P}]^{\mathrm{T}}[A]^{-1}[\bar{P}][Y_1]\{Z_1\} - [Y_1]^{\mathrm{T}}[\bar{P}]^{\mathrm{T}}[A]^{-1}[\bar{P}][S_k]\{R(t)\}$$

which should be regarded as a non-linear one, because the number of rows of the matrix $[\bar{P}]$ depends upon the displacements $\{Z_1\}$, $\{Z_2\}$. The dimension of equation (40) equals the length of the vector $\{Z_1\}$. The modal displacements $\{Z_2\}$ at each time point are obtained from the second equation of (38).

So we have shown that in the above-presented dynamic reduction approach, a unilaterally constrained structure is represented by a dynamic equation with a non-linear term and, consequently, conventional numerical integration schemes can be employed. In such a way a compromise between the dynamic model accuracy and computational efficiency can be achieved. Moreover, in the case of reduced models, only unilateral constraints upon the displacements are to be imposed while the impact velocity restitution conditions are governed by the compliance of the truncated modes. As the term $[Y_1]^{\mathrm{T}}[\bar{P}]^{\mathrm{T}}[A]^{-1}[\bar{P}][Y_1]$ on the left-hand side of equation (40) can be regarded as representing the stiffness coefficients of unilateral springs, elastic impact conditions are implied.

The accuracy of the approximation can be improved by retaining the term $[\mathrm{diag}(\mu_2)]\{\dot{Z}_2\}$ in the second equation of (38). It has been shown in Reference 7 that

$$\begin{aligned}
\{\lambda(Z_1, \dot{Z}_1)\} = [A]^{-1}([P][Y_1]\{Z_1\} + [B_1][A]^{-1}[P][Y_1]\{\dot{Z}_1\} \\
- \{d_0\} + [P][S_k]\{R\}) \qquad (41)
\end{aligned}$$

where $[B_1] = [P][S_{D1}][P]^{\mathrm{T}}$, $[S_{D1}] = [Y_2][\mathrm{diag}(\mu_2/\omega_2^2)][Y_2]^{\mathrm{T}}$, and the values of the components of the vector $\{\lambda\}$ obtained by the relation (41) are modified by means of the relation

$$\lambda_i = \begin{cases} \lambda_i & \text{if the value } \lambda_i > 0 \text{ has been obtained from (39) and from (41) simultaneously,} \\ 0 & \text{if the reverse is true.} \end{cases}$$

Presenting the reduced dynamic equation in a form similar to equation (40), we obtain, on the left-hand side, the terms representing unilateral stiffness and damping elements and therefore in this case viscoelastic impact conditions are implied.

4. NUMERICAL RESULTS

4.1. Free longitudinal impact vibrations of a beam vibroconverter (VC)

We consider finite element models of different discretization levels, Figure 2. If the number of elements NEL = 1, the model presents a mass attached to a spring, and by increasing the number of elements the dynamic behaviour of a continuous VC is approximated. In an undeformed state, the constraint coincides with the right-hand end of the VC. At the initial state the VC is considered as being compressed by force F_n, and at the time point $t = 0$ it is released by removing the force F_n. The time laws of the displacements of the model during the free vibroimpact motion depend upon the number of elements of the model, as well as, upon the local contact conditions.

The computed results are presented in terms of the following dimensionless quantities: the displacement of the right-hand end $\bar{U}_n = U_n/U_0$, the time $\bar{t} = t/T_0$, the impetus of normal contact interaction forces $\bar{S} = S/k_0 U_0 T_0$, where U_0 is the initial displacement of the right-hand end owing to the initial compression of the VC by the force F_n, T_0 is the period of the first mode of the impact free vibration of the VC, k_0 is the longitudinal stiffness of the VC. The rheological model of the contact interaction pair is presented by the spring of stiffness $\bar{k} = k/k_0$ and the viscous damping element $\bar{c} = c/kT_0$ connected in parallel.

Figure 3 illustrates the action of the numerical scheme by presenting the time laws of the displacements $\bar{U}_n$ and of the normal contact force impetus $\bar{S}$ of the single-d.o.f. model at different values of the velocity restitution coefficient. The obtained time laws are practically identical to the corresponding exact solutions. The time laws of the models of several discretization levels at the values of the velocity restitution coefficient $R_f = 0$ and $R_f = 1$ are presented in Figure 4. The internal damping in the VC is assumed to be very small. At $R_f = 0$ the energy dissipation level is high, and the accumulated impetus of contact forces is significantly lower than at $R_f = 1$, because at $R_f = 0$ kinetic energy is lost during plastic impacts of the point mass at the right-hand end of the model. The larger amount of mass of the structure is concentrated at the contact point, the more energy is lost at each impact, the greater is the rate of a total energy decrease (if NEL = 1, the energy equals zero after the very first impact). By increasing the number of elements, i.e. by approaching nearer the continuous model of the VC, motion laws become less dependent upon the velocity restitution coefficient R_f. If $R_f > 0$, each impact presents a series of microimpacts

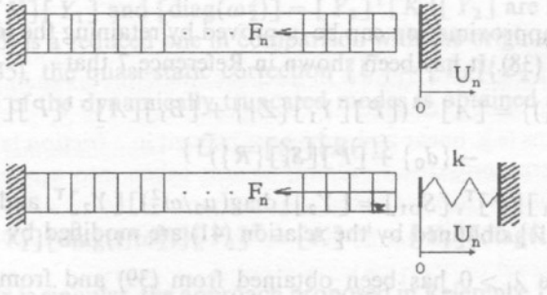

Figure 2. Finite element models of a vibroconverter

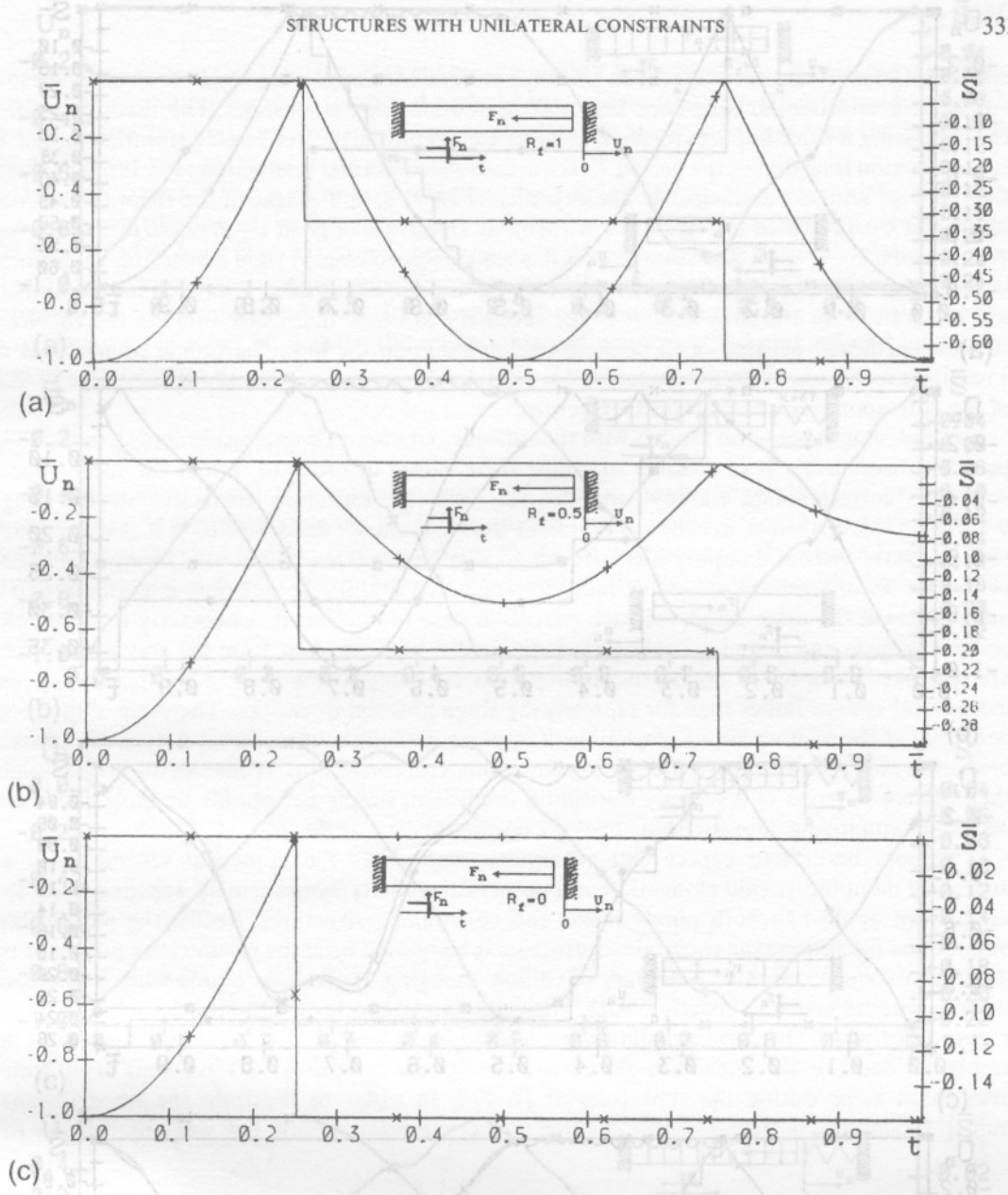

Figure 3. Free motion laws of the displacements and the interaction force impetus of the right-hand end of the one-element model (NEL = 1), a local contact condition being prescribed in terms of a velocity restitution coefficient R_f: (+) $\bar{U}_n$; (×) $\bar{S}$; (a) $R_f = 1$, (b) $R_f = 0{\cdot}5$, (c) $R_f = 0$

(quasi-plastic impact).[17] It follows that in general an impact of an elastic structure is always elastic, independent of the velocity restitution coefficient in the vicinity of a local contact area.

Free impact vibrations have been investigated by employing the rheological contact interaction models, Figure 2(b). Figure 5 shows the time laws of the displacements and of the accumulated normal interaction force impetus at various values of the rheology stiffness coefficient $\bar{k}$. It follows from the comparison of the obtained results that by increasing the rheology stiffness

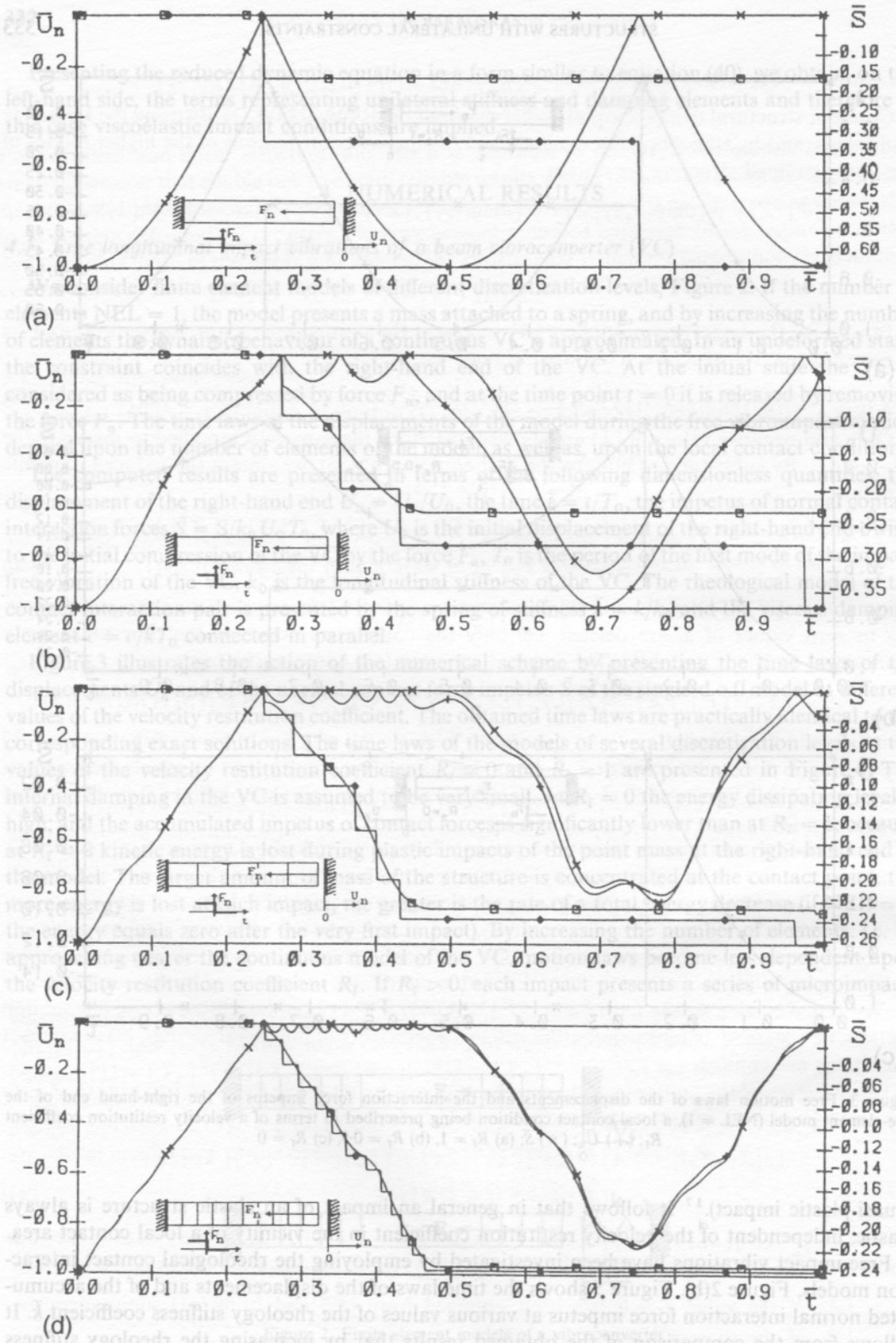

Figure 4. Free motion laws of the displacements and the interaction force impetus of the right-hand end of the model, a local contact condition being prescribed in terms of a velocity restitution coefficient R_f: (+) $\bar{U}_n$ at $R_f = 0$; ($\diamond$) $\bar{S}$ at $R_f = 0$; ($\times$) $\bar{U}_n$ at $R_f = 1$, ($\square$) $\bar{S}$ at $R_f = 1$; (a) NEL = 1, (b) NEL = 2, (c) NEL = 5, (d) NEL = 10

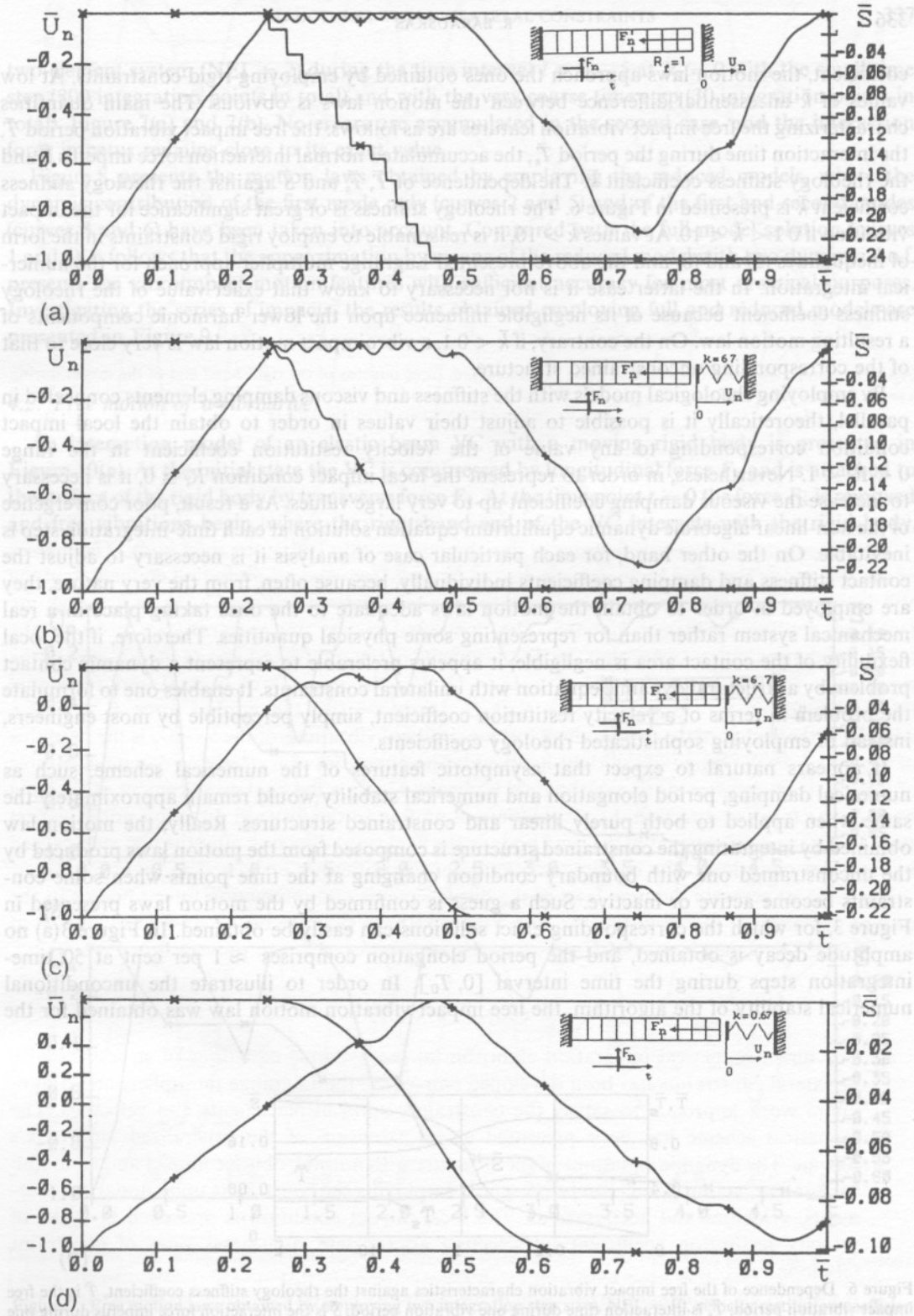

Figure 5. Free motion laws of the displacements and the interaction force impetus of the right-hand end of the model, a local contact condition being prescribed in terms of rheology stiffness coefficient $\bar{k}$, NEL = 10: (+) $\bar{U}_n$; (×) $\bar{S}$; (a) rigid constraint, $R_f = 1$, (b) $\bar{k} = 67$, (c) $\bar{k} = 6{\cdot}7$, (d) $\bar{k} = 0{\cdot}67$

coefficient, the motion laws approach the ones obtained by employing rigid constraints. At low values of $\bar{k}$ an essential difference between the motion laws is obvious. The main quantities characterizing the free impact vibration features are as follows: the free impact vibration period $\bar{T}$, the interaction time during the period $\bar{T}_s$, the accumulated normal interaction force impetus $\bar{S}$ and the rheology stiffness coefficient $\bar{k}$. The dependence of $\bar{T}$, $\bar{T}_s$ and $\bar{S}$ against the rheology stiffness coefficient $\bar{k}$ is presented in Figure 6. The rheology stiffness is of great significance for the impact vibration if $0{\cdot}1 < \bar{k} < 10$. At values $\bar{k} > 10$, it is reasonable to employ rigid constraints in the form of inequalities (2) and (8) and the above-presented Lagrange multiplier approach for the numerical integration. In the latter case it is not necessary to know that exact value of the rheology stiffness coefficient because of its negligible influence upon the lower harmonic components of a resulting motion law. On the contrary, if $\bar{k} < 0{\cdot}1$, a vibroimpact motion law is very close to that of the corresponding unconstrained structure.

By employing rheological models with the stiffness and viscous damping elements connected in parallel, theoretically it is possible to adjust their values in order to obtain the local impact condition corresponding to any value of the velocity restitution coefficient in the range $0 < R_f < 1$. Nevertheless, in order to represent the local impact condition $R_f \cong 0$, it is necessary to increase the viscous damping coefficient up to very large values. As a result, poor convergence of the non-linear algebraic dynamic equilibrium equation solution at each time-integration step is inevitable. On the other hand, for each particular case of analysis it is necessary to adjust the contact stiffness and damping coefficients individually, because often, from the very nature, they are employed in order to obtain the motion laws adequate to the ones taking place in a real mechanical system rather than for representing some physical quantities. Therefore, if the local flexibility of the contact area is negligible, it appears preferable to represent a dynamic contact problem by a structural dynamic equation with unilateral constraints. It enables one to formulate the problem in terms of a velocity restitution coefficient, simply perceptible by most engineers, instead of employing sophisticated rheology coefficients.

It appears natural to expect that asymptotic features of the numerical scheme, such as numerical damping, period elongation and numerical stability would remain approximately the same when applied to both purely linear and constrained structures. Really, the motion law obtained by integrating the constrained structure is composed from the motion laws produced by the unconstrained one with boundary condition changing at the time points when some constraints become active or inactive. Such a guess is confirmed by the motion laws presented in Figure 3, for which the corresponding exact solutions can easily be obtained. In Figure 3(a) no amplitude decay is obtained, and the period elongation comprises ≈ 1 per cent at 50 time-integration steps during the time interval $[0, T_0]$. In order to illustrate the unconditional numerical stability of the algorithm, the free impact vibration motion law was obtained for the

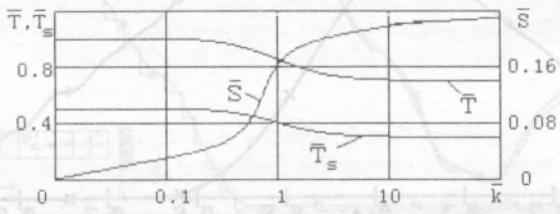

Figure 6. Dependence of the free impact vibration characteristics against the rheology stiffness coefficient, $\bar{T}$ is the free impact vibration period; $\bar{T}_s$ is interaction time during one vibration period; $\bar{S}$ is the interaction force impetus during one vibration period

two-element system (NEL = 2) during the time interval $\bar{t} = 0 - 5$ at $R_f = 0$ with the small time step (800 integration points in total) and with the very coarse time step (30 integration points in total), Figure 7(a) and 7(b). No errors are accumulated in the second case, and the interaction force impetus remains close to its exact value.

Figure 8 presents the motion laws obtained by employing the reduced models, where the dynamic contribution of the first mode only (curves 2 and 5) and of the first and second modes (curves 3 and 6) have been taken into account. Compared with the full-model solution (curves 1 and 4), it follows that the approximation by means of the reduced model with two dynamic d.o.f. presents the vibroimpact motion features with sufficient accuracy for most practical purposes. Investigating the series of impacts, the results obtained employing full and reduced models are presented in Figure 9.

4.2. Free motion of a vibrodrive

An interaction model of an elastic beam VC with a moving rigid body is presented in Figure 10(a). At the initial state the VC is compressed by longitudinal force F_x and is attached to the surface of the rigid body by transverse force F_y. At the time point $t = 0$ the force F_x is removed and free vibrations begin, where the right-hand end of the VC interacts with the rigid body.

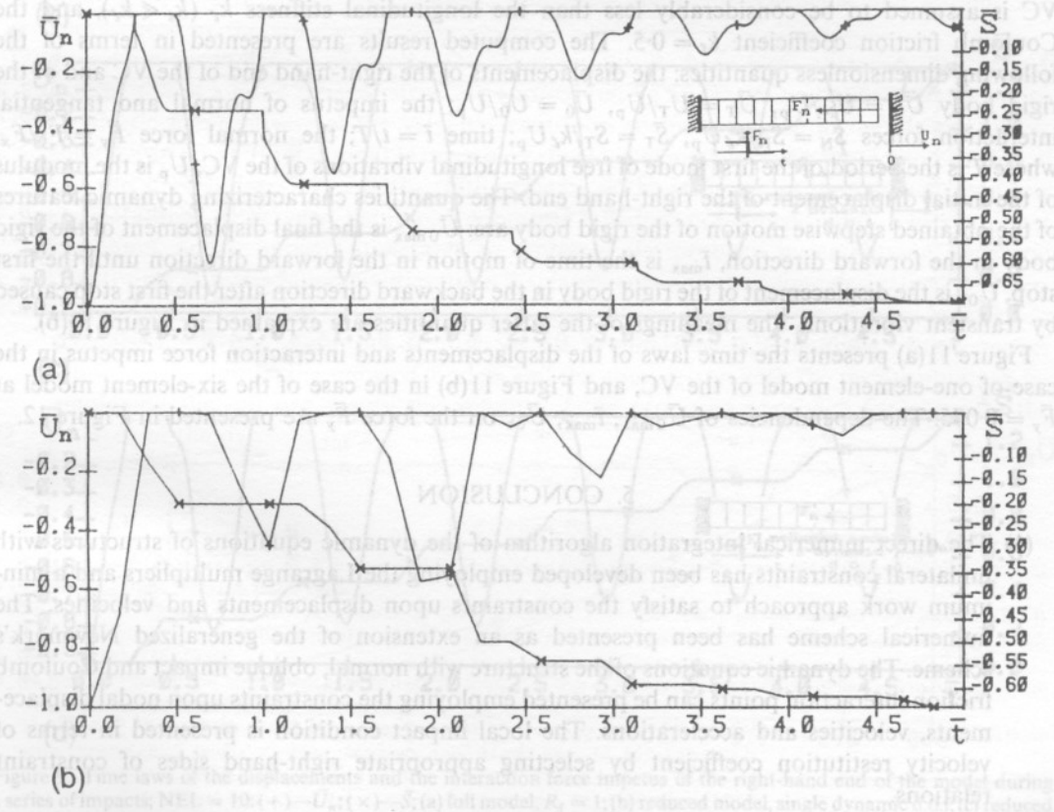

Figure 7. Free motion laws obtained by employing two integration step sizes, NEL = 10, velocity restitution coefficient $R_f = 0$, number of integration steps: (+) $\bar{U}_n$; (×) $\bar{S}$; (a) 800 integration points, (b) 30 integration points

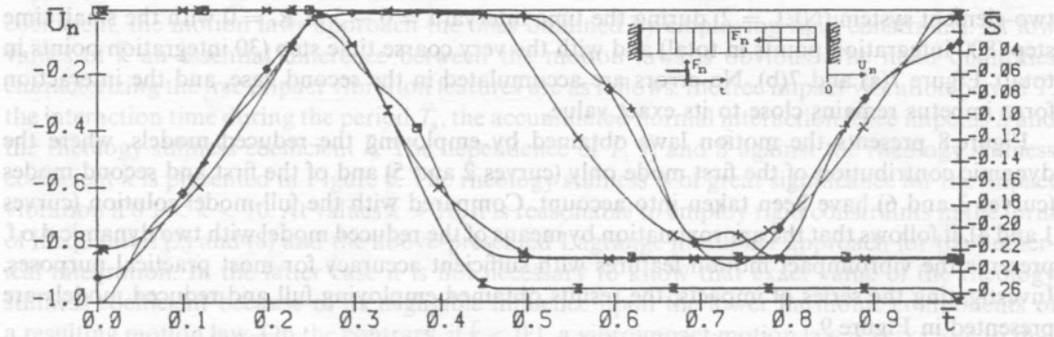

Figure 8. Time laws of the displacements and the interaction force impetus of the right-hand end of the model during a single impact; NEL = 10: (+) $\bar{U}_n$; (□) $\bar{S}$—full model, $R_f = 0$; (×) $\bar{U}_n$; (╳) $\bar{S}$— reduced model, single dynamic d.o.f, (◇) $\bar{U}_n$; (⋈) $\bar{S}$—reduced model, two dynamic d.o.f.

Because of the normal and tangential contact interaction forces the rigid body begins to move. After some time vibrations cease, and the system comes to a state of rest.

We investigate the dynamic features of the obtained motion law of the rigid body. The masses of the VC and of the rigid body are assumed to be equal ($m = m_0$) the bending stiffness k_s of the VC is assumed to be considerably less than the longitudinal stiffness k_ℓ ($k_s \ll k_\ell$), and the Coulomb friction coefficient $k_f = 0{\cdot}5$. The computed results are presented in terms of the following dimensionless quantities: the displacements of the right-hand end of the VC and of the rigid body $\bar{U}_N = U_N/U_p$, $\bar{U}_T = U_T/U_p$, $\bar{U}_0 = U_0/U_p$; the impetus of normal and tangential interaction forces $\bar{S}_N = S_N/k_\ell U_p$, $\bar{S}_T = S_T/k_\ell U_p$; time $\bar{t} = t/T$; the normal force $\bar{F}_y = F_y/F_x$, where T is the period of the first mode of free longitudinal vibrations of the VC, U_p is the modulus of the initial displacement of the right-hand end. The quantities characterizing dynamic features of the obtained stepwise motion of the rigid body are: $\bar{U}_{0\max}$ is the final displacement of the rigid body in the forward direction, $\bar{t}_{\max}$ is the time of motion in the forward direction until the first stop, $\bar{U}_{0b}$ is the displacement of the rigid body in the backward direction after the first stop caused by transient vibrations. The meanings of the latter quantities are explained in Figure 10(b).

Figure 11(a) presents the time laws of the displacements and interaction force impetus in the case of one-element model of the VC, and Figure 11(b) in the case of the six-element model at $\bar{F}_y = 0{\cdot}075$. The dependencies of $\bar{U}_{0\max}$, $\bar{t}_{\max}$, $\bar{U}_{0b}$ on the force $\bar{F}_y$ are presented in Figure 12.

5. CONCLUSION

(1) The direct numerical integration algorithm of the dynamic equations of structures with unilateral constraints has been developed employing the Lagrange multipliers and a minimum work approach to satisfy the constraints upon displacements and velocities. The numerical scheme has been presented as an extension of the generalized Newmark's scheme. The dynamic equations of the structure with normal, oblique impact and Coulomb friction interaction points can be presented employing the constraints upon nodal displacements, velocities and accelerations. The local impact condition is presented in terms of velocity restitution coefficient by selecting appropriate right-hand sides of constraint relations.

(2) A method for the dynamic reduction of unilaterally constrained elastic structures has been developed based upon the representation of the model equations in modal co-ordinates of

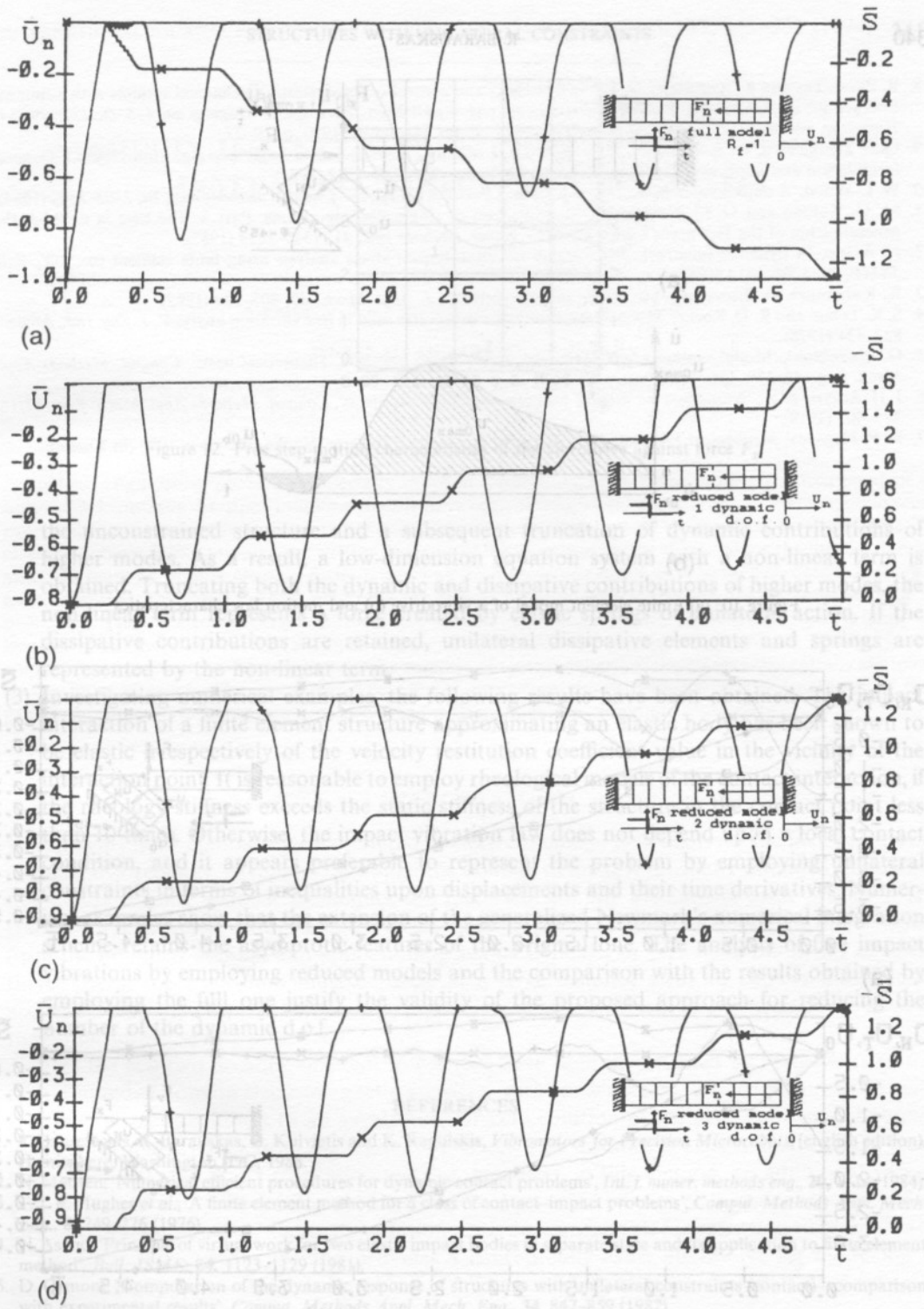

Figure 9. Time laws of the displacements and the interaction force impetus of the right-hand end of the model during a series of impacts; NEL = 10: (+)—$\bar{U}_n$; (×)—$\bar{S}$; (a) full model, $R_f = 1$; (b) reduced model, single dynamic d.o.f; (c) reduced model, two dynamic d.o.f; (d) reduced model, three dynamic d.o.f.;

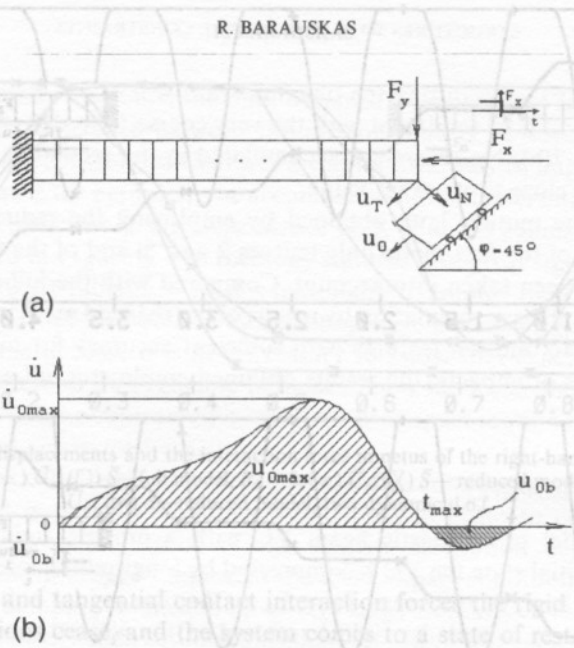

Figure 10. (a) Finite element model of a vibrodrive (b) and motion law characteristics

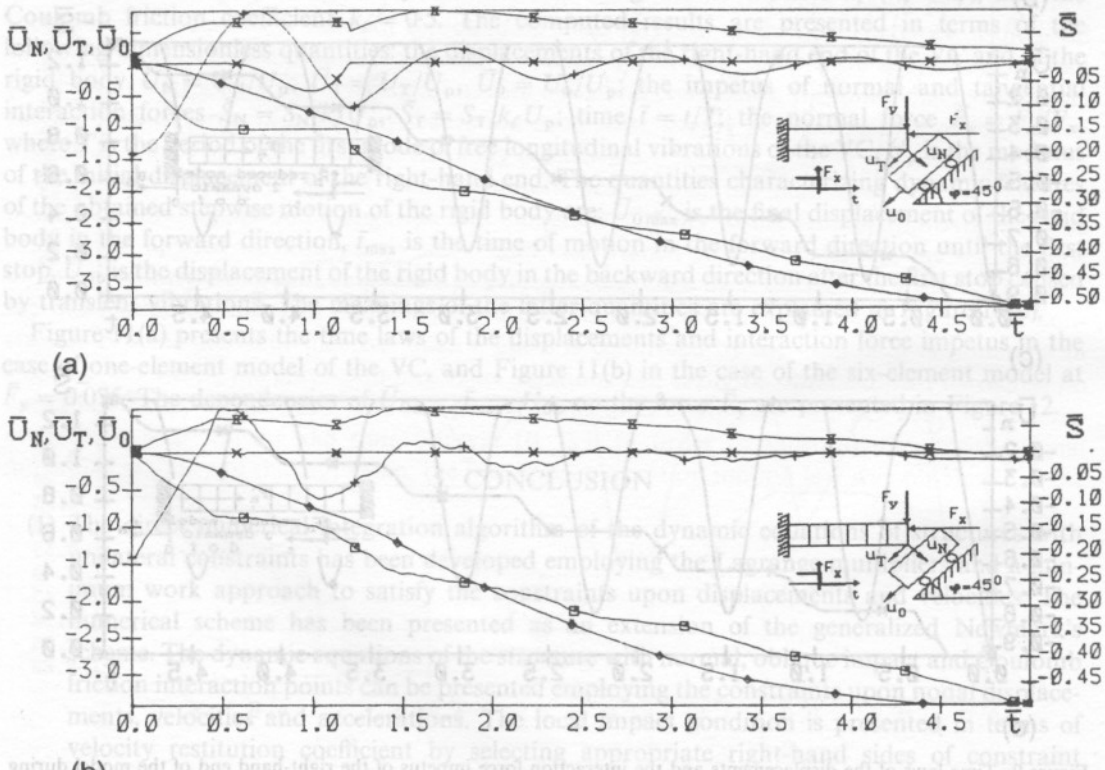

Figure 11. Free step-motion laws of the displacements and of the interaction force impetus of the right-hand end of the vibrodrive at $\bar{F}_y = 0{\cdot}075$, $m = m_0$, $k_s \ll k_\ell$, $k_f = 0{\cdot}5$; (a) NEL = 1; (b) NEL = 6; (+) $\bar{U}_N$; (×) $\bar{U}_T$; (◇) $\bar{U}_T$; (□) $\bar{S}_N$; (⊠) $\bar{S}_T$

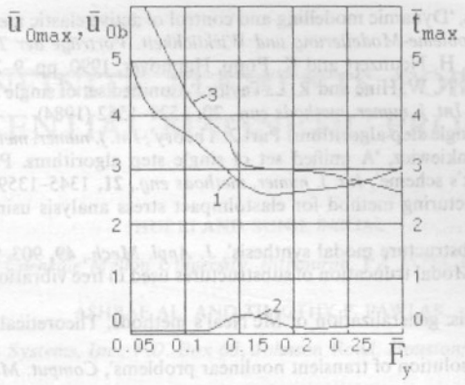

Figure 12. Free step-motion characteristics of the vibrodrive against force F_y

the unconstrained structure and a subsequent truncation of dynamic contributions of higher modes. As a result, a low-dimension equation system with a non-linear term is obtained. Truncating both the dynamic and dissipative contributions of higher modes, the non-linear term represents a force created by elastic springs of unilateral action. If the dissipative contributions are retained, unilateral dissipative elements and springs are represented by the non-linear term.

(3) Investigating numerical examples, the following results have been obtained. The impact interaction of a finite element structure approximating an elastic body has been shown to be elastic irrespectively of the velocity restitution coefficient value in the vicinity of the interaction point. It is reasonable to employ rheological models of the contact interaction, if the rheology stiffness exceeds the static stiffness of the structure in the contact point less than 10 times. Otherwise, the impact vibration law does not depend upon a local contact condition, and it appears preferable to represent the problem by employing unilateral constraints in terms of inequalities upon displacements and their time derivatives. Numerical examples show that the extension of the generalized Newmark's numerical integration scheme retains the asymptotic features of the original one. The analysis of free impact vibrations by employing reduced models and the comparison with the results obtained by employing the full one justify the validity of the proposed approach for reducing the number of the dynamic d.o.f.

REFERENCES

1. R. Bansevicius, R. Barauskas, G. Kulvietis and K. Ragulskis, *Vibromotors for Precision Microrobots*, (english edition), Hemisphere, Washington, DC, 1988.
2. N. Madsen, 'Numerical efficient procedures for dynamic contact problems', *Int. j. numer. methods eng.*, **20,** 1–14 (1984).
3. T. J. R. Hughes *et al.*, 'A finite element method for a class of contact–impact problems', *Comput. Methods Appl. Mech. Eng.*, **8,** 249–276 (1976).
4. N. Asano, 'Principle of virtual work for two elastic impact bodies in separate state and its application to finite element method', *Bull. JSME*, **24,** 1123–1129 (1981).
5. D. Osmont, 'Computation of the dynamic response of structures with unilateral constraints (contact)—comparison with experimental results', *Comput. Methods Appl. Mech. Eng.*, **34**, 847–859 (1982).
6. D. Talaslidis, ' A linear finite element approach to the solution of the variational inequalities arising in contact problems of structural dynamics', *Int. j. numer. methods eng.*, **18,** 1505–1520 (1982).
7. R. Barauskas, *Dynamic Analysis and Synthesis of Elastic Structures with Unilateral Constraints. Computer Methods and Application to Controlled Vibrational Systems*, Technologija, Kaunas, 1992.

8. R. Barauskas and K. Ragulskis, 'Dynamic modelling and control of active elastic mechanical systems with nonlinear interaction', in *Dynamische Probleme-Modelierung und Wirklichkeit. Vorträge der Tagung am 4–5 October 1990 in Hannover*, editors H. G. Natte, H. Neunzert and K. Popp, Hannover, 1990, pp. 9–27.
9. O. C. Zienkiewicz, W. L. Wood, N. W. Hine and R. L. Taylor, 'A unified set of single step algorithms. Part 1. General formulation and applications', *Int. j. numer. methods eng.*, **20,** 1529–1552 (1984).
10. W. L. Wood, 'A unified set of single step algorithms. Part 2. Theory', *Int. j. numer. methods eng.*, **20,** 2303–2309 (1984).
11. M. G. Katona and O. C. Zienkiewicz, 'A unified set of single step algorithms. Part 3. The beta-*m* method, the generalization of the Newmark's scheme', *Int. j. numer. methods eng.*, **21,** 1345–1359 (1985).
12. N. Asano, 'A dynamic substructuring method for elastoimpact stress analysis using finite element method', *Bull. JSME*, **26,** 1308–1314 (1983).
13. K. Kubomura, 'A theory of substructure modal synthesis', *J. Appl. Mech.*, **49,** 903–909 (1982).
14. S. K. Tolani and R. D. Rocke, 'Modal truncation of substructures used in free vibration analysis', *J. Eng. Ind.*, August, 827–834 (1976).
15. G. Rosenblum, 'Modal synthesis: generalization of Mc'Neal's methods. Theoretical basis', *Comput. Methods Appl. Mech. Eng.*, **48,** 139–154 (1985).
16. J. H. Argyris *et al.*, 'Numerical solution of transient nonlinear problems', *Comput. Methods Appl. Mech. Eng.*, **17/18,** 341–409 (1979).
17. R. F. Nagayev, *Mechanical Processes with Repeated Dying down Impacts*, Nauka, Moscow, 1985 (in Russian).